Polym. Bull. (2012) 68:1815–1829
DOI 10.1007/s00289-011-0652-3

ORIGINAL PAPER

Synthesis and properties of triblock copolymers containing PDMS via AGET ATRP

Yue Sun · Weiqu Liu

Received: 25 May 2011 / Revised: 9 August 2011 / Accepted: 7 October 2011 /
Published online: 15 October 2011

Abstract The bromo-terminated macroinitiator was prepared by direct addition reaction of difunctional poly(dimethylsiloxane) (PDMS) containing methyl methacrylate end groups with hydrobromic acid in acetic acid under mild conditions, and well-defined triblock copolymers of poly(methyl methacrylate-*b*-dimethylsiloxane-*b*-methyl methacrylate) (MMA-*b*-DMS-*b*-MMA) were synthesized via activators generated by election transfer atom transfer radical polymerization (AGET ATRP). The gel permeation chromatography data obtained verified the polymerization and showed the well controlling of the reaction. FTIR and ^{1}H NMR measured the structure of the macroinitiator and copolymers. The contact angle measurement indicated that the water contact angles decreased gradually with the increasing of PMMA block content. The self-assembly behaviors of the triblock polymer were studied by transmission electron micrograph, scanning electron microscopy, and dynamic light scattering measurement. The results indicated that the polymers could self-assemble into various complex morphologies in different solvents and the morphologies depended on the properties of solvents. The possible molecular packing models for self-assembly behaviors of the ABA triblock polymers were proposed.

Keywords PDMS · Triblock copolymer · AGET ATRP · Self-assembly

Y. Sun · W. Liu (✉)
Guangzhou Institute of Chemistry, Chinese Academy of Sciences, Guangzhou 510650, China
e-mail: liuwq@gic.ac.cn

Y. Sun
Graduate School of Chinese Academy of Sciences, Beijing 100049, China

Introduction

Poly(dimethylsiloxane) (PDMS) and their composite materials have received great attention due to their unique properties, such as low glass transition temperature, low surface energy, good water repellency, and excellent biocompatibility [1–3]. However, because of its awful film-forming property, poor cohesion, and higher cost, its application is limited. Poly(methyl methacrylate) (PMMA) is a biocompatible material that has good chemical and mechanical resistances [4]; meanwhile, it is characterized by lower cost, good cohesiveness, and excellent film-forming property [5]. Thus, a considerable amount of work has been undertaken to enhance the properties of PDMS by PMMA.

Block copolymers have unique microphase separation, which make them have broad application including compatibilizers, surfactants, dispersants, emulsifiers, foam stabilizers, drug delivery, and templates for functional materials [6–8]. Block copolymers prepared from PDMS and PMMA will have not only the advantages of both the two materials but also the properties of block copolymers. Many techniques have been used to synthesize block copolymers, atom transfer radical polymerization (ATRP) is one of the most robust and efficient method, yielding well-defined copolymers with precisely controlled topology, composition, and functionality [9, 10]. Various block copolymers containing PDMS and PMMA have been prepared via ATRP [11–13]. However, normal ATRP is sensitive to oxygen and its catalyst concentration is independently reduced [14], which greatly impede the use of ATRP in the commercial production of block copolymers. In order to overcome the drawbacks, an improved ATRP technique, activators generated by election transfer ATRP (AGET ATRP) was proposed by Matyjaszewski and co-workers [15]. In which the active catalyst Cu (I) is generated in situ by the reaction between the air-stable Cu (II) species and a reducing agent [16]. Thus, all agents can be thoroughly mixed in the presence of air, and the reducing agent can be added at a controlled rate [17]. In short, AGET ATRP has the advantages of facile preparation, storage, and handling of catalysts [18]. It is becoming one of the most powerful, versatile, simple, and inexpensive methods in living/controlled free radical polymerization [14]. To the best of our knowledge, the studies about block copolymers prepared from PDMS and PMMA via AGET ATRP have been seldom reported.

PDMS was usually converted into macroinitiator and used in ATRP. For example, Connal and Qiao [19] prepared an effective PDMS macroinitiator for ATRP via the reaction of monohydroxyl-terminated PDMS with 2-bromoisobutyryl bromide. Miller and Matyjaszewski [11] synthesized mono- and difunctional PDMS macroinitiators and used them to initiate the ATRP of (meth)acrylates. Rached et al. [20] proposed a new PDMS macroinitiator by an original synthesis scheme in two steps, which involved the scarcely reported reaction of isocyanates with silanol groups. Hydrogen bromide dissolved in ethanoic acid is an attractive, commercially available, inexpensive reagent that appears to duplicate gaseous HBr chemistry and deserves to be more widely known [21]. The use of this mixture for performing hydrobrominations has a long history but appears to have been overlooked by many scientists.

Considering that AGET ATRP have more advantages than normal ATRP on commercial prospects and the advantages of hydrobromic acid in acetic acid, in this

article, the bromo-terminated macroinitiator was prepared by direct addition reaction of difunctional PDMS containing methyl methacrylate end groups with hydrobromic acid in acetic acid under mild conditions, and the well-defined ABA triblock copolymers of poly(methyl methacrylate-*b*-dimethylsiloxane-*b*-methyl methacrylate) (MMA-*b*-DMS-*b*-MMA) were synthesized via AGET ATRP. The gel permeation chromatography (GPC) data obtained verified the polymerization and showed the well controlling of the reaction. FTIR and ^{1}H NMR measured the structures of the macroinitiator and triblock copolymers. The contact angles measurement investigated the surface properties of triblock copolymers, then transmission electron micrograph (TEM), scanning electron microscopy (SEM), and dynamic light scattering (DLS) showed the self-assembly behaviors of the polymers in pure solvent of acetone, tetrahydrofuran (THF), and toluene because of their different polarity. Finally, the possible molecular packing models for self-assembly behaviors of the polymers were proposed.

Experimental

Materials

Difunctional PDMS containing methyl methacrylate end groups was purchased from Shanghai silicone Co. Ltd. (Shanghai, China). Methyl methacrylate (MMA), acetone, THF, and toluene were obtained from Kemiou Chemical Co. (Tianjin, China). Hydrobromic acid in acetic acid (saturation) was supplied by King Success fine Chemical Co. Ltd. (Hubei, China). 2,2′-Bipyridine (Bpy) and copper (0) powder were from Alfa Aesar Chemical Co. Copper (II) bromide, butanone, and benzoyl peroxide (BPO)were purchased from Zhenxin Chemical Co. Ltd. (Shanghai, China).

All chemicals used were without further purification. All solvents were reagent grade.

Sample preparation

Preparation of the macroinitiator of bromo-terminated PDMS

PDMS (20 g), BPO (0.5 g), hydrobromic acid in acetic acid (200 mL), and 100 mL acetone were put into a 500-mL three-necked flask, which was fitted with a mechanical stirrer, a thermometer, and an apparatus for dealing with tail gas (HBr). Then, the reaction mixture was stirred at 0 °C. After 10 h, the production was extracted by water and toluene until the pH of the oil liquid is 7.0. Finally, excess solvent was thoroughly removed by a rotary evaporator under vacuum.

Synthesis of poly(MMA-b-DMS-b-MMA) by AGET ATRP

The PDMS macroinitiator was first dissolved in the mixture of toluene and butanone in a 100-mL three-necked flask equipped with a mechanical stirrer, a thermometer, and an inlet system of nitrogen. Then the reagent with a molar ratio MMA/$CuBr_2$/

bpy = 100/0.1/0.2 was injected into the reaction flask. After the reaction mixture was thoroughly purged by vacuum and flushed with nitrogen three times, the flask was immersed in an oil bath at 95 °C. Finally, Cu (0) powder (with a molar ratio $CuBr_2$/Cu (0) = 0.1/0.2) was added to initiate the polymerization of MMA. After 9 h, the reaction was stopped and quickly cooled down to room temperature. The product poly(MMA-*b*-DMS-*b*-MMA) was obtained after precipitation in water, filtration, and drying under high vacuum to constant weight.

Characterization

The GPC measurements were carried out on a Waters 515-410 instrument at 35 °C with THF as the solvent (1.0 mL/min) and polystyrene as the calibration standards.

The FTIR spectra were recorded on a WQF 410 Spectrophotometer made in Beijing, China.

^{1}H NMR was performed on a 400 MHz Brüker NMR spectrometer (Model DRX-400) using $CDCl_3$ as solvent and tetramethylsilane as an internal reference. Chemical shifts of the ^{1}H NMR were related to the $CDCl_3$ signal at 7.24 ppm.

The contact angle of water was measured on the air-side surface of the coating films with a contact goniometer (Erma Contact Anglemeter, Model G-I, 13-100-0, Japan) by the sessile drop method with a micro-syringe at 30 °C. The sample was prepared by casting the polymer onto a clean glass disk from 20% (w/w) solution of butanone. The disk was put into an oven at 60 °C for 12 h and 60 °C for 12 h under vacuum. More than 10 readings were averaged to get a reliable value for each sample.

TEM and SEM images were obtained by JEM-100CXII at 200 kV and Philips/FEI XL-30 with an accelerating voltage of 20 kV, respectively. For observation of the size and morphology of the copolymer aggregates, ABA triblock copolymers was dissolved in acetone, THF, and toluene to make a series of polymer solutions at the concentrations of 1 wt%. A small drop of the solution was deposited onto a copper TEM grid covered with carbon film, and then the solution was dried at atmospheric pressure and room temperature.

DLS (Brookhaven Zeta Pals) determined the diameters of the aggregates in solution.

Results and discussion

The synthesis of PDMS macroinitiator and poly(MMA-*b*-DMS-*b*-MMA)

As shown in Scheme 1, PDMS transformed into a macroinitiator by direct addition reaction of difunctional PDMS containing methyl methacrylate end groups with hydrobromic acid in acetic acid, and then the macroinitiator initiated the polymerization of MMA to get triblock copolymers of poly(MMA-*b*-DMS-*b*-MMA). The AGET ATRP data for the polymerization and the composition of a series of copolymers were obtained and listed in Table 1. As can be seen, the low PDI were achieved and the reactions were well controlled.

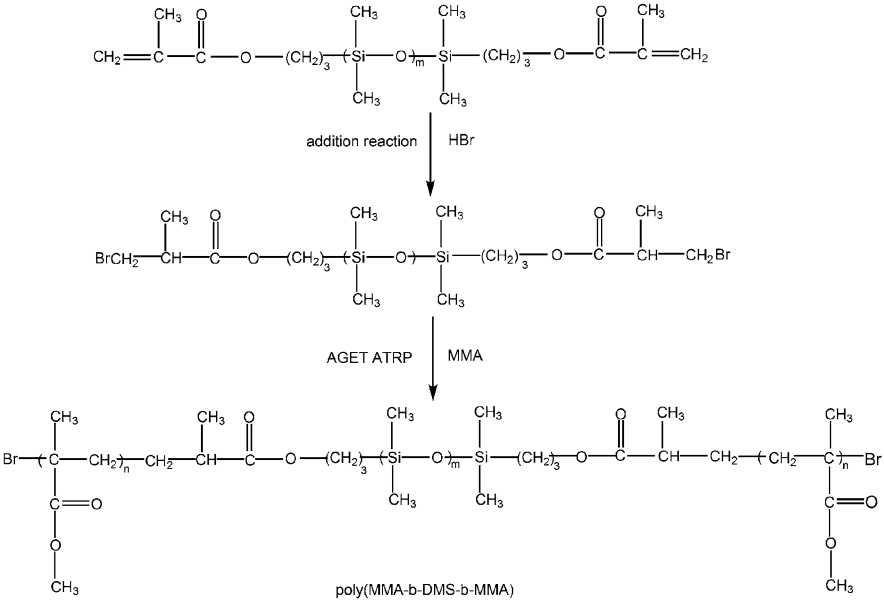

Scheme 1 The preparation of macroinitiator Br-PDMS-Br and the synthesis of triblock copolymer via AGET ATRP

The typical molecular weight distributions for Br-PDMS-Br and poly(MMA-*b*-DMS-*b*-MMA) are shown in Fig. 1. The elution time for poly(MMA-*b*-DMS-*b*-MMA) was shorter than that for Br-PDMS-Br, showing that its molecular weight was larger than that of Br-PDMS-Br. The monomodal GPC curve of the copolymer suggested the formation of block copolymer without homopolymerization. No observable peak of the macroinitiator from the GPC curve of the block copolymer indicated the complete initiation of the macroinitiator.

The characterization of PDMS macroinitiator and poly(MMA-*b*-DMS-*b*-MMA)

The structures of the macroinitiator and poly(MMA-*b*-DMS-*b*-MMA) were analyzed by FT-IR and ^{1}H NMR data. Figure 2 showed the FT-IR spectra of difunctional PDMS containing methyl methacrylate end groups (trace a), Br-PDMS-Br (trace b), and poly(MMA-*b*-DMS-*b*-MMA) (trace c). Trace a and trace b were very similar, they both exhibited the characteristic peaks at 1260 cm^{-1} (Si–CH_3), 1000–1100 cm^{-1} (Si–O–Si asymmetric stretching vibration), and 800 cm^{-1} (Si–O asymmetric stretching vibration) from PDMS [22]. Comparing trace a with trace b, unambiguous disappearance of the characteristic peak of C=C at 1635 cm^{-1} (trace a) and the appearance of the characteristic peak of C–Br at 568 cm^{-1} (trace b) were observed, this indicated the completion of the direct addition reaction and the successful preparation of the macroinitiator. Figure 2c revealed that the copolymer consists of PMMA and PDMS. The characteristic spectra of PDMS, Si–CH_3 in 1260 cm^{-1}, Si–O–Si in 1000–1100 cm^{-1}, Si–O in 800 cm^{-1}, still existed. The

Table 1 The AGET ATRP data for the polymerization and the composition of a series of copolymers

Sample	[MMA]:[PDMS][a]		Conv[c]	Mn[d]	PDI[d]	Composition of the polymer[e]
	Before reaction	In the polymer obtained[b]				
1	0:100	0:100	–	4012	1.15	Br-PDMS$_{48}$-Br
2	15:85	13.8:86.2	91	4600	1.19	PMMA$_3$-*b*-PDMS$_{48}$-*b*-PMMA$_3$
3	30:70	27.9:72.1	90	5620	1.20	PMMA$_8$-*b*-PDMS$_{48}$-*b*-PMMA$_8$
4	50:50	47.2:52.8	89	7630	1.21	PMMA$_{18}$-*b*-PDMS$_{48}$-*b*-PMMA$_{18}$
5	65:35	62.3:37.7	89	10630	1.22	PMMA$_{33}$-*b*-PDMS$_{48}$-*b*-PMMA$_{33}$
6	85:15	83.5:16.5	89	23820	1.22	PMMA$_{101}$-*b*-PDMS$_{48}$-*b*-PMMA$_{101}$

[a] The data were the relative weight ratios

[b] The data were determined by ^{1}H NMR

[c] The monomer conversion was determined gravimetrically

[d] The number-average molecular weight (Mn) and the polydispersity index (PDI) were obtained by GPC

[e] The numbers of repeat units of MMA and DMS were determined from GPC data

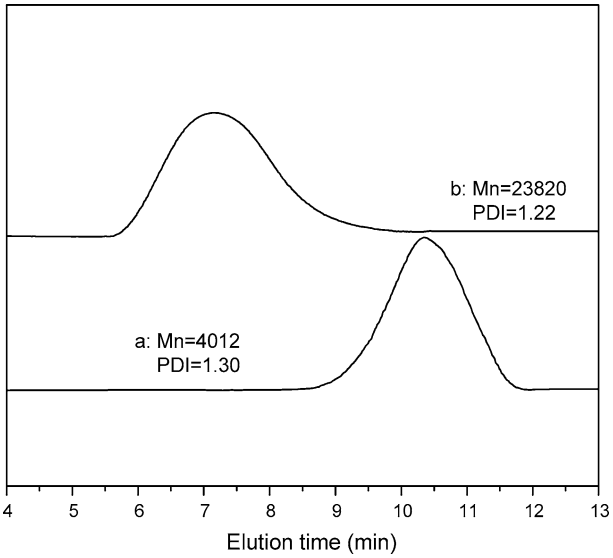

Fig. 1 The typical GPC traces of the macroinitiator Br-PDMS-Br (*a*) and the block copolymer poly(MMA-*b*-DMS-*b*-MMA) (*b*)

peaks of PMMA appeared at 2951, 1732, 1449, and 1159 cm^{-1} were assigned to C–H stretching, C=O stretching, CH_3 stretching, and –O–CH_3 stretching vibrations, respectively [23].

Figure 3 showed the ^{1}H NMR spectra of Br-PDMS-Br (A) and poly(MMA-*b*-DMS-*b*-MMA) (B). In trace (A), the sharp peak at 0.15 ppm was attributed to the Si–CH_3 (a, b) protons in PDMS segments. Peaks at 0.33 and 1.94 ppm were designated to Si–CH_2 (c) and –CH_2 (d), and peaks at 1.33 and 3.83 ppm were

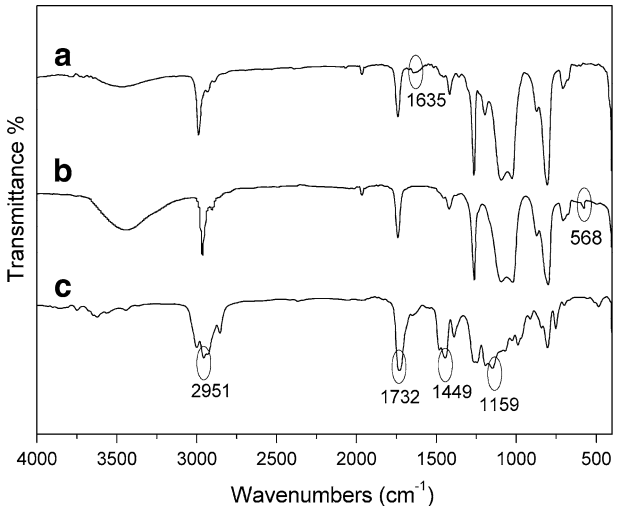

Fig. 2 FT-IR spectra of PDMS (*a*), macroinitiator Br-PDMS-Br (*b*), and poly(MMA-*b*-DMS-*b*-MMA) (*c*)

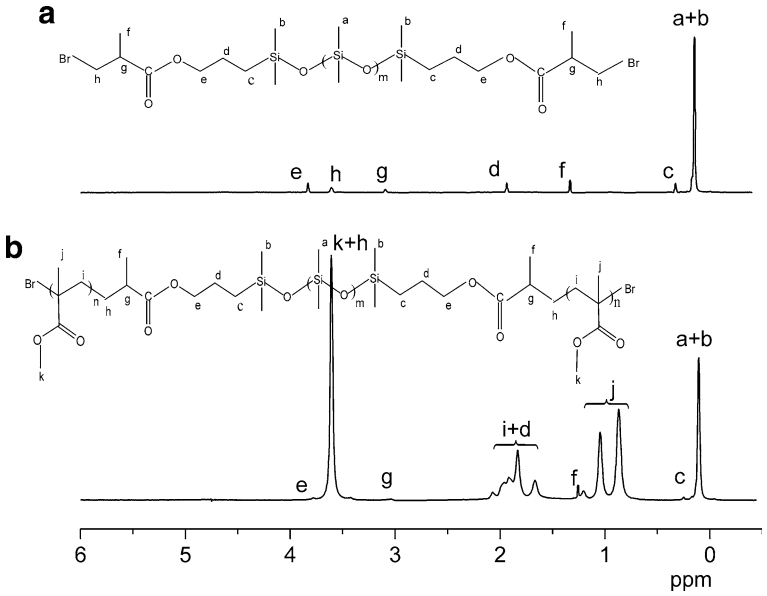

Fig. 3 ^{1}H NMR spectra of Br-PDMS-Br (**A**) and poly (MMA-*b*-DMS-*b*-MMA) (**B**)

corresponding to $-CH_3$ (f) and $-CH_2OCO$ (e), while peaks at 3.09 and 3.60 ppm were corresponding to –CH (g) and $-CH_2$ (h) [24, 25]. In trace (B), all the peaks of Br-PDMS-Br could be observed, and the peaks of $-CH_2$ (i), $-CH_3$ (j), and $-OCH_3$ (k) at 1.61–2.08, 0.78–1.22, and 3.56–3.67 ppm, respectively, due to PMMA

Table 2 The content of MMA, contact angle and the surface energy of the series of polymers

Sample	Copolymer	Content of MMA[a] (%)	Contact angle[b] (°)	γ_S^c (mN/m)
1	Br-$PDMS_{48}$-Br	0	105.0	20.1
2	$PMMA_3$-*b*-$PDMS_{48}$-*b*-$PMMA_3$	13.8	102.1	21.8
3	$PMMA_8$-*b*-$PDMS_{48}$-*b*-$PMMA_8$	27.9	100.3	22.9
4	$PMMA_{18}$-*b*-$PDMS_{48}$-*b*-$PMMA_{18}$	47.2	98.0	24.3
5	$PMMA_{33}$-*b*-$PDMS_{48}$-*b*-$PMMA_{33}$	62.3	95.8	25.7
6	$PMMA_{101}$-*b*-$PDMS_{48}$-*b*-$PMMA_{101}$	83.5	92.5	27.7

[a] The data determined by ^{1}H NMR

[b] The water contact angle on the air-side surface of the copolymers films

[c] Surface energy obtained indirectly from the water contact angle

segments could be clearly seen [25]. From the FTIR and ^{1}H NMR spectra, poly(MMA-*b*-DMS-*b*-MMA) was synthesized successfully via AGET ATRP.

Surface properties of the block copolymers

The water contact angles of the copolymer films were measured to demonstrate the effect of PMMA on the surface properties of triblock copolymers, and the data are shown in Table 2. As expected, PMMA increased the wettability of PDMS and the water contact angles toward the air-side surface of the copolymer films decreased gradually with the increasing of PMMA block content. It was interested in using these materials as biocompatible materials, since PDMS was a hydrophobic material, and it would be desirable to lower the contact angle to obtain a material that can be better accommodated to the biocompatible materials [26].

Surface energies of the copolymers were indirectly obtained from static water contact angles. An equation of $1 + \cos\theta = 2(\gamma_S/\gamma_L)^{1/2}\exp[-\beta(\gamma_L - \gamma_S)^2]$ was applied to calculate the surface energy [27, 28]. β was a constant with a value of 0.0001247 $(m^2/mJ)^2$ [28]; θ, γ_S, and γ_L were the contact angle, the surface energy of the solid, and the surface energy of the tested liquid, respectively. The results in Table 2 showed that the surface energies of polymers increased with the increase of PMMA content. Especially, when the PMMA content were 83.5% (sample 6 of Table 2), the surface energy of the polymer film increased to 27.7 mN/m, which was much higher than that of PDMS (20.1 mN/m). All the results of surface energy were agreeable with the contact angle measurements.

Self-assembly behaviors of poly(MMA-*b*-DMS-*b*-MMA)

The self-assembly behavior of block copolymers in selective solvents was one of their important properties, which was a basic element for their variety of applications. The different morphologies self-assembled from the same copolymers would have different applications. It was reported that the solvent was one of

important morphogenic factors, since polymer–solvent interactions determined the coil dimensions of each block [29, 30].

In order to study the influence of solvent on the self-assembly behavior of poly(MMA-*b*-DMS-*b*-MMA), acetone, THF, and toluene were used as the structural-directing solvent because of their different polarity. Figure 4 showed the TEM and SEM images formed from $PMMA_{101}$-*b*-$PDMS_{48}$-*b*-$PMMA_{101}$ in different solvent. We found that the rod micelles with degree of branching could be prepared when acetone was as a structural directing agent (Fig. 4a, d). TEM results showed the average diameter of the micelles was ~50–150 nm. When THF used as a solvent, we could see the dominant morphology was giant vesicles and some of them aggregated together (Fig. 4b and e, respectively). The TEM image also revealed the inner structure of the vesicles, it can be seen that the vesicles had

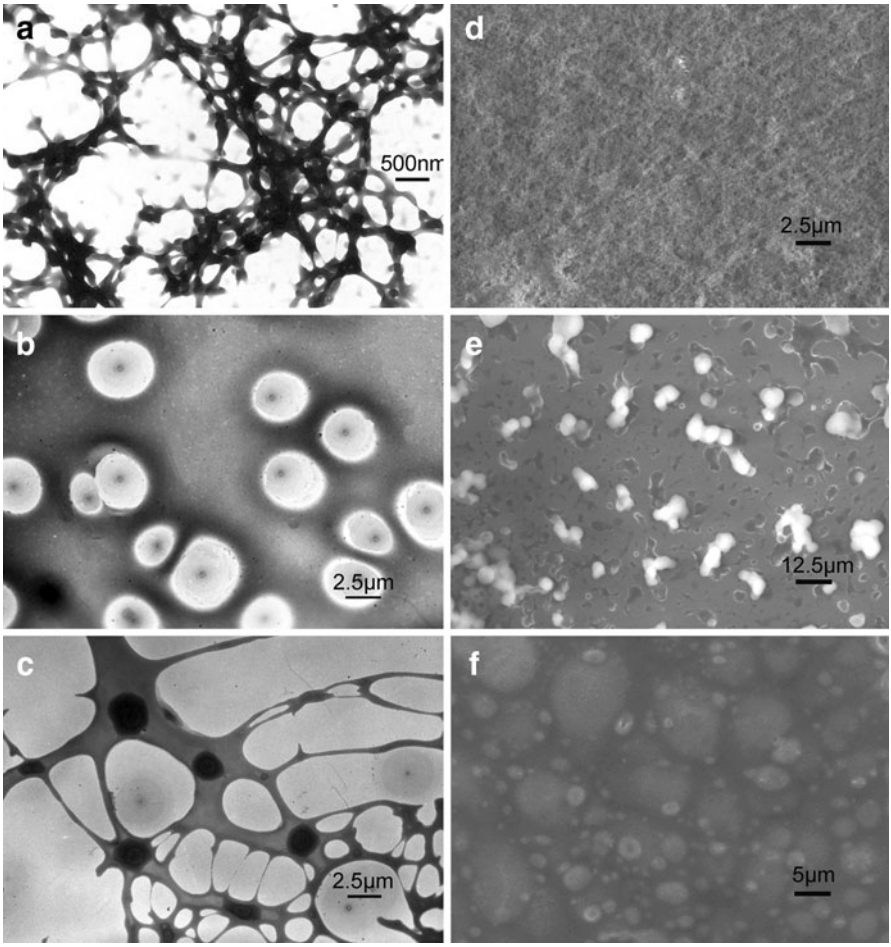

Fig. 4 $PMMA_{101}$-*b*-$PDMS_{48}$-*b*-$PMMA_{101}$ self-assembly in different solvents. TEM images of **a** acetone, **b** THF, **c** toluene and SEM images of **d** acetone, **e** THF, and **f** toluene

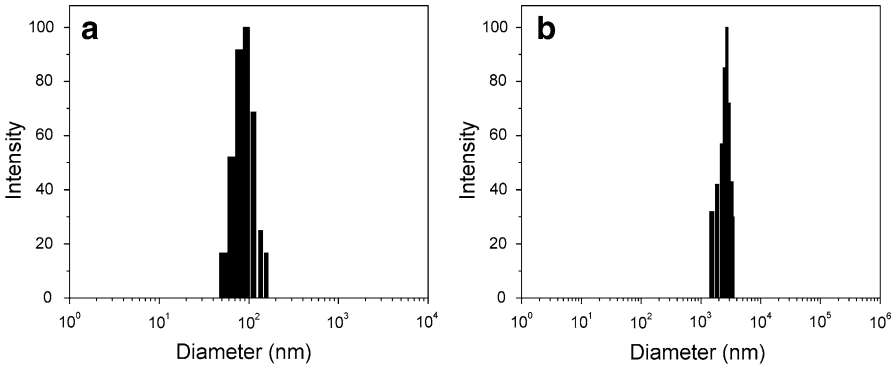

Fig. 5 DLS measurement of $PMMA_{101}$-*b*-$PDMS_{48}$-*b*-$PMMA_{101}$ in the solution of acetone (**a**) and toluene (**b**)

core–shell structures and there was a black dot in every core. The core diameter was about ~5.5 μm and the shell diameter was about 8.5 μm (Fig. 4b). When the solvent was toluene, one example of a trapped intermediate morphology was shown by TEM and SEM images (Fig. 4c, f). The TEM image (Fig. 4c) gave the clear inner structure of the intermediate morphology, which was the transition between the vesicles with core–shell and the connected rodlike micelles, i.e., some vesicles with rods extending from the edge (Fig. 4c). The core diameter of the vesicles was about 0.5–1.5 μm and the shell diameter was about 1.5–3.5 μm. From Fig. 4, the properties of solvent was a key factor to influence the self-assembly behavior of amphiphilic molecules.

From Fig. 4, the diameters of the aggregates were very large, one may doubt the block copolymers did not self-assemble, and the morphologies shown in the images just resulted from the films of the polymer precipitated on the copper TEM grid. Thus, DLS experiments were performed to further investigate the aggregation behavior of $PMMA_{101}$-*b*-$PDMS_{48}$-*b*-$PMMA_{101}$ in different solvents and the results are shown in Fig. 5. As can be seen, the diameters of the micelles formed from $PMMA_{101}$-*b*-$PDMS_{48}$-*b*-$PMMA_{101}$ in acetone solution were ranging from 55 to 156 nm (Fig. 5a), which was larger than that measured by TEM. The reason for that may be because the DLS measurements were carried out in solution where the corona of the aggregates would stretched out to some extent due to the solubility in the toluene, while the TEM measurements were made on the solid aggregates in which the corona were collapsed [31]. Unfortunately, DLS did not give effective results of the polymers in THF solution although the same set of experiments was performed many times. It is known that the range of the particle size from Brookhaven Zeta Pals was 1 nm to 6 μm. DLS results may indirectly indicate that the diameters of the aggregates formed from the polymer in THF were very large in the solution and they were above 6 μm. Figure 5b shows the size distribution of the aggregates formed from the polymers in toluene solution, the range of the diameters was 1.5–3.5 μm, which were consistent with the results of TEM. From the results of DLS, the conclusion may be drawn that the morphologies shown in the TEM and

Table 3 The solubility parameter (δ) and the dielectric constant (ε) of the solvent and polymers [36–40]

	Solubility parameter $(MJ/m^3)^{1/2}$	Dielectric constant (F/m)
Acetone	20.3	20.7
THF	18.6	7.58
Toluene	18.2	2.24
PMMA	19.4	3.15
PDMS	14.9–15.6	2.65

SEM did not result from the films of the polymer precipitated on the copper TEM grid.

It is well known that several factors influence the morphology of block copolymer aggregates in a solution [32, 33]. For example, the interaction of inter-coronal chain, the core–coronal interfacial energy, and the degree of core-chain stretching. The factors mentioned above can be predicted from some parameters, named the solubility parameter δ and the dielectric constant ε [30]. The closer the match between the solubility parameter of the solvent and that of the core-forming block, the higher the solvent content of the core and the higher the degree of stretching of the core chains. The lower the polarity of the solvent, the weaker the corona–solvent interaction and the weaker the repulsive interactions among the corona chains; this increased the aggregation number and degree of stretching in the core [34, 35].

To understand the morphology mechanism of $PMMA_{101}$-*b*-$PDMS_{48}$-*b*-$PMMA_{101}$ in different solvents, in this article, the solubility parameter δ and the dielectric constant ε of the blocks in the polymer and solvents were searched and are listed in Table 3. Comparing the data of the solubility parameter δ in Table 3, acetone, THF, and toluene could be considered good solvent for PMMA blocks, and poor solvent for PDMS block. However, the difference of the solubility parameter (δ) and the dielectric constant (ε) for the three solvents may cause the different morphologies of $PMMA_{101}$-*b*-$PDMS_{48}$-*b*-$PMMA_{101}$ in solution.

A tentative schematic representation of $PMMA_{101}$-*b*-$PDMS_{48}$-*b*-$PMMA_{101}$ aggregates in different solvent is shown in Scheme 2. As for the copolymers acetone was a good solvent for PMMA blocks, but a poor solvent for PDMS blocks. The amphiphilic block copolymers of $PMMA_{101}$-*b*-$PDMS_{48}$-*b*-$PMMA_{101}$ would undergo self-assembly in acetone to form aggregates of a core–shell structure driven by the attractive forces between the molecules and the repulsive forces that prevent the initial growth of the aggregate [30, 41]. It should be stressed that the core of the aggregates was formed from the PDMS blocks and the corona of the aggregates should be composed of the PMMA blocks (Scheme 2a). Meanwhile, the corona-forming blocks were much longer than the core-forming blocks and that was the so-called star micelles. The star micelles were usually spherical, because the repulsive interactions among the corona chains were strong, due to the relatively high density of corona chains on the core surface [42]. Nonspherical micelles in solutions had been observed only rarely, and mostly indirectly. For example, it was reported rodlike or cylindrical micelles existed in systems of polystyrene-*b*-poly(methyl

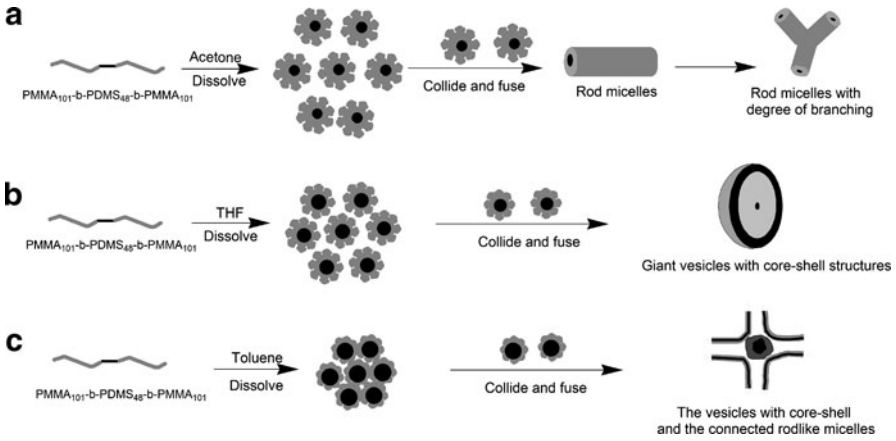

Scheme 2 Proposed molecular packing models for the self-assembly of $PMMA_{101}$-*b*-$PDMS_{48}$-*b*-$PMMA_{101}$ in different solvents. **a** acetone, **b** THF, and **c** toluene

methacrylate) in mixed solvents and polystyrene-*b*-poly(4-vinylpyridine) in dilute solution, depending on the block copolymer composition[33, 43, 44]. According to above results, those small spheres formed from $PMMA_{101}$-*b*-$PDMS_{48}$-*b*-$PMMA_{101}$ maybe just an intermediate and would collide, fuse, and undergo a secondary aggregation to form rod micelles with degree of branching under the copolymer composition of this article. The schematic representation of the high degree branching of micelles shown in Scheme 2a.

Scheme 2b showed the possible schematic descriptions of $PMMA_{101}$-*b*-$PDMS_{48}$-*b*-$PMMA_{101}$ aggregates in THF, which was also the selective solvent for PMMA blocks. The amphiphilic block copolymers of $PMMA_{101}$-*b*-$PDMS_{48}$-*b*-$PMMA_{101}$ would also undergo self-assembly to form aggregates of a core–shell structure. The core of the aggregates was formed from the PDMS blocks and the corona of the aggregates was composed of the PMMA blocks as well. However, the solubility parameters of THF ($\delta = 18.6$ $(MJ/m^3)^{1/2}$) were closer to that of PDMS ($\delta = 14.9$–15.6 $(MJ/m^3)^{1/2}$) than was the solubility parameter of acetone ($\delta = 20.3$ $(MJ/m^3)^{1/2}$) (see Table 3), the degree of swelling of the micelle core, and consequently the degree of core-chain stretching increased when THF was used as the solvent instead of acetone [33, 37]. The solvent nature affected the strength of corona chain repulsion as well. In a solvent with a low dielectric constant such as THF ($\varepsilon = 7.58$ F/m), the corona–solvent interaction and the repulsive interactions among the corona chains were expected to be lower than in the case of acetone, which have higher dielectric constants ($\varepsilon = 20.7$ F/m) (see Table 3) [30, 34]. Consequently, the electrostatic repulsion among corona chains decreased when acetone were replaced by THF. Since aggregates prepared in THF, experienced a higher degree of core-chain stretching, and a lower intercorona repulsion than those prepared in acetone, a stronger driving force to reduce the total free energy of the system occured in that order and caused the increasing of the aggregation number, thus a series of giant vesicles may be got in the case of THF.

Scheme 2c was the possible schematic descriptions of the copolymers aggregates in toluene and the morphology mechanism was similar to that mentioned above. From the data in Table 3, when toluene was used as the solvent instead of THF, the match between the solubility parameter of the solvent and that of the aggregates core (PDMS) would be closer, the solvent content of the core (PDMS) and the degree of stretching of PDMS chains would be higher. At the same time, because of the lower polarity of toluene, the corona–solvent interaction and the repulsive interactions among the corona chains would be weaker; this would increase the aggregation number and degree of stretching of PDMS in the core [34]. As a result, multiple morphologies (transition between the vesicles with core–shell and the connected rodlike micelles) were trapped.

Conclusion

A bromo-terminated macroinitiator was synthesized by direct addition reaction of difunctional PDMS containing methyl methacrylate end groups with hydrobromic acid in acetic acid. Then the macroinitiator initiated the polymerization of MMA to form well-defined ABA triblock copolymers of poly(MMA-*b*-DMS-*b*-MMA) via AGET ATRP. GPC data obtained verified the polymerization and showed the well controlling of the reaction. FTIR and ^{1}H NMR measured the structures of the macroinitiator and its triblock copolymers. The water contact angles of the copolymer films was measured to demonstrate the effect of PMMA on the surface properties of triblock copolymers, and the results indicated that the water contact angles decreased gradually with the increasing of PMMA block content. Then the self-assembly behaviors of the triblock polymer were studied by TEM, SEM, and DLS measurement. It was found that the polymers could self-assemble into various complex morphologies in different solvents, including rod micelles with degree of branching, giant vesicles with core–shell structures and the transition between the vesicles and the connected rodlike micelles. The TEM results indicated that the morphologies of the polymers depended on the properties of solvents. The possible molecular packing models for self-assembly behaviors of the ABA triblock polymers were proposed as well. The results suggested that the ABA triblock polymers containing PDMS would have applications for drug delivery systems, encapsulation, and so on.

Acknowledgments Authors gratefully acknowledge the financial support from the Guangdong Natural Science Foundation, China (No: 07006841) and the open project of Key Laboratory of Cellulose and Lignocellulosics Chemistry, Chinese Academy of Sciences (No: LCLC-2010-11).

References

1. Lim T, Webber E, Johnston P (1999) Synthesis and characterization of poly(dimethyl siloxane)-poly[alkyl(meth)acrylic acid] block copolymers. Macromolecules 32:2811–2815
2. Deng B, Luo R, Chen H, Liu B, Feng Y, Sun Y (2007) Synthesis and surface properties of PDMS–acrylate emulsion with gemini surfactant as co-emulsifier. Colloid Polym Sci 285:923–930

3. Bes L, Huan K, Khoshdel E, Lowe M, McConville C, Haddleton D (2003) Poly(methylmethacrylate-dimethylsiloxane) triblock copolymers synthesized by transition metal mediated living radical polymerization: bulk and surface characterization. Eur Polym J 39:5–13
4. Bruens M, Pieterman H, Wijn J, Vaandrager J (2003) Porous polymethylmethacrylate as bone substitute in the craniofacial area. J Craniofac Surg 14:63–68
5. Chen H, Deng X, Hou X, Luo R, Liu B (2009) Preparation and characterization of PDMS-PMMA interpenetrating polymer networks with indistinct phase separation. J Macromol Sci A 46:83–89
6. Shi Z, Holdcroft S (2004) Synthesis of block copolymers possessing fluoropolymer and non-fluoropolymer segments by radical polymerization. Macromolecules 37:2084–2089
7. Xu S, Liu W (2008) Synthesis of amphiphilic fluorinated copolymer and the formation of hollow nanotubes. Colloids Surf A 326:210–213
8. Chen Q, Zhao H, Ming T, Wang J, Wu C (2009) Nanopore extrusion-induced transition from spherical to cylindrical block copolymer micelles. J Am Chem Soc 131:16650–16651
9. Wang JS, Matyjaszewski K (1995) Controlled/"living" radical polymerization. Halogen atom transfer radical polymerization promoted by a Cu(I)/Cu(II) redox process. Macromolecules 28:7901–7910
10. Dong H, Matyjaszewski K (2010) Thermally responsive p($M(EO)_2$MA-co-OEOMA) copolymers via AGET ATRP in miniemulsion. Macromolecules 43:4623–4628
11. Miller P, Matyjaszewski K (1999) Atom transfer radical polymerization of (meth) acrylates from poly(dimethylsiloxane) macroinitiators. Macromolecules 32:8760–8767
12. Huan K, Bes L, Haddleton D, Khoshdel E (2001) Synthesis and properties of polydimethylsiloxane-containing block copolymers via living radical polymerization. J Polym Sci A 39:1833–1842
13. Brown D, Price G (2001) Preparation and thermal properties of block copolymers of PDMS with styrene or methyl methacrylate using ATRP. Polymer 42:4767–4771
14. Chen H, Liang Y, Liu D, Tan Z, Zhang S, Zheng M, Qu R (2010) AGET ATRP of acrylonitrile with ionic liquids as reaction medium without any additional ligand. Mater Sci Eng C 30:605–609
15. Min K, Gao H, Matyjaszewski K (2005) Preparation of homopolymers and block copolymers in miniemulsion by ATRP using activators generated by electron transfer (AGET). J Am Chem Soc 127:3825–3830
16. Li Q, Zhang L, Zhang Z, Zhou N, Cheng Z, Zhu X (2010) Air-tolerantly surface-initiated AGET ATRP mediated by iron catalyst from silica nanoparticles. J Polym Sci A 48:2006–2015
17. Qian H, He L (2009) Surface-initiated activators generated by electron transfer for atom transfer radical polymerization in detection of DNA point mutation. Anal Chem 81:4536–4542
18. Hu Z, Shen X, Qiu H, Lai G, Wu J, Li W (2009) AGET ATRP of methyl methacrylate with poly(ethylene glycol) (PEG) as solvent and TMEDA as both ligand and reducing agent. Eur Polym J 45:2313–2318
19. Connal L, Qiao G (2006) Preparation of porous poly(dimethylsiloxane)-based honeycomb materials with hierarchal surface features and their use as soft-lithography templates. Adv Mater 18:3024–3028
20. Rached R, Hoppe S, Jonquieres A, Lochon P, Pla F (2006) A new macroinitiator for the synthesis of triblock copolymers PA_{12}-b-PDMS-b-PA_{12}. J Appl Polym Sci 102:2818–2831
21. Brown T, Dronsfield A, Ellis R (1990) The addition of hydrogen bromide to unsymmetrical alkenes: introductory experiments in NMR spectroscopy and mechanistic chemistry. J Chem Educt 67:518
22. Feng L, Fang H, Zhou S, Wu L (2006) One-Step method for synthesis of PDMS-based macroazo-initiators and block copolymers from the initiators. Macromol Chem Phys 207:1575–1583
23. Ramesh S, Leen K, Kumuth K, Arof A (2007) FTIR studies of PVC/PMMA blend based polymer electrolytes. Spectrochim Acta A 66:1237–1242
24. Ma S, Liu W, Yu D, Wang Z (2010) Modification of epoxy resin with polyether-grafted-polysiloxane and epoxy-miscible polysiloxane particles. Macromol Res 18:22–28
25. Emmanuel D, Jean H, Philippe D, Philippe D (2006) Synthesis of silicone-methacrylate copolymers by ATRP using a nickel-based supported catalyst. Macromol Chem Phys 207:1116–1125
26. Anjos D, Revoredo E, Galembeck A (2010) Silicone-polyacrylate chemical compatibilization with organosilanes. Polym Eng Sci 50:606–612
27. Luo Z, He T, Yu H, Dai L (2008) A novel ABC triblock copolymer with very low surface energy: poly(dimethylsiloxane)-block-poly(methyl methacrylate)-block- poly(2,2,3,3,4,4,4-heptafluorobutyl methacrylate). Macromol React Eng 2:398–406
28. Li D, Neumann A (1990) A reformulation of the equation of state for interfacial tensions. J Colloid Interface Sci 137:304–307

29. Förster S, Zisenis M, Wenz E, Antonietti M (1996) Micellization of strongly segregated block copolymers. J Chem Phys 104:9956–9970
30. Riegel I, Samios D, Petzhold C, Eisenberg A (2003) Self-assembly of amphiphilic di and triblock copolymers of styrene and quaternized 5-(N,N-diethylamino) isoprene in selective solvents. Polymer 44:2117–2128
31. Terreau O, Luo L, Eisenberg A (2003) Effect of poly(acrylic acid) block length distribution on polystyrene-b-poly(acrylic acid) aggregates in solution. 1. Vesicles. Langmuir 19:5601–5607
32. Zhang L, Eisenberg A (1998) Formation of crew-cut aggregates of various morphologies from amphiphilic block copolymers in solution. Polym Adv Technol 9:677–699
33. Zhang L, Eisenberg A (1996) Multiple morphologies and characteristics of "crew-cut" micelle-like aggregates of polystyrene-b-poly(acrylic acid) diblock copolymers in aqueous solutions. J Am Chem Soc 118:3168–3181
34. Yu Y, Zhang L, Eisenberg A (1998) Morphogenic effect of solvent on crew-cut aggregates of amphiphilic diblock copolymers. Macromolecules 31:1144–1154
35. Ma R, Ma RM, Feng L, Fan L, Liu Y, Xing B, Hou Y, Bao F (2009) The synthesis of P(MAn-co-St)-b-PS-b-P(MAn-co-St) block copolymers by RAFT polymerization and the nanostructure of their self-assembly aggregates. Colloids Surf A 346:184–194
36. Kawagoe M, Ishimi T (2002) On the properties of organic liquids affecting the crazing behaviour in glassy polymers. J Mater Sci 37:5115–5121
37. Choucair A, Eisenberg A (2003) Control of amphiphilic block copolymer morphologies using solution conditions. Eur Phys J E 10:37–44
38. Lai C, Lee H, Hu C (2005) Theoretical study on the mechanism of *N*-heterocyclic carbene catalyzed transesterification reactions. Tetrahedron Lett 46:6265–6270
39. Stafie N, Stamatialis DF, Wessling M (2004) Insight into the transport of hexane–solute systems through tailor-made composite membranes. J Membr Sci 228:103–116
40. Chiang C, Lin C, Ju M (2007) An implantable capacitive pressure sensor for biomedical applications. Sensor Actuat A 134:382–388
41. Zhang L, Shen H, Eisenberg A (1997) Phase separation behavior and crew-cut micelle formation of polystyrene-b-poly(acrylic acid) copolymers in solutions. Macromolecules 30:1001–1011
42. Zhang L, Eisenberg A (1999) Thermodynamic vs kinetic aspects in the formation and morphological transitions of crew-cut aggregates produced by self-assembly of polystyrene-b-poly(acrylic acid) block copolymers in dilute solution. Macromolecules 32:2239–2249
43. Antonietti M, Heinz S, Schmidt M, Rosenauer C (1994) Determination of the micelle architecture of polystyrene/poly(4-vinylpyridine) block copolymers in dilute solution. Macromolecules 27: 3276–3281
44. Utiyama H, Takenaka K, Mizumori M, Fukuda M, Tsunashima Y, Kurata M (1974) Light-scattering studies of a polystyrene-poly(methyl methacrylate) two-block copolymer in mixed solvents. Macromolecules 7:515–520